PHYSICAL REVIEW D **79,** 034017 (2009)

CP asymmetry in the decays $B \to (X_s, X_d)\mu^+\mu^-$ with four generations

Ashutosh Kumar Alok,* Amol Dighe,† and Shamayita Ray‡

Tata Institute of Fundamental Research, Homi Bhabha Road, Mumbai 400005, India

(Received 8 December 2008; published 18 February 2009)

We estimate the *CP* asymmetry $A_{CP}(q^2)$ in the decays $B \to X_s\mu^+\mu^-$ and $B \to X_d\mu^+\mu^-$ in the standard model (SM) with an additional fourth generation. We use a parametrization that allows us to explore the complete parameter space of the 4×4 quark mixing matrix, and constrain these parameters from the current data on B decays. We find that the enhancement in $A_{CP}(q^2)$ depends strongly on the mass of the t', the up-type quark in the fourth generation. For $m_{t'}$ around 400 GeV, the *CP* asymmetry in the high-q^2 region ($q^2 > 14.4$ GeV^2) can be enhanced by more than an order of magnitude for $B \to X_s\mu^+\mu^-$ and up to a factor of 6 for $B \to X_d\mu^+\mu^-$. There is no enhancement in the low-q^2 region ($1 < q^2 < 6$ GeV^2). With increasing $m_{t'}$, $A_{CP}(q^2)$ in the high-q^2 (low-q^2) region first decreases (increases) and then saturates at a value a few times the SM prediction. In the high-q^2 region of $B \to X_s\mu^+\mu^-$, this saturation value may be up to 25 times the SM expectation.

DOI: 10.1103/PhysRevD.79.034017 PACS numbers: 13.20.He

I. INTRODUCTION

Upcoming high statistics experiments at the LHC and super-B factories will provide stringent tests of the standard model (SM) via flavor physics involving B decays. The large number of B hadrons anticipated to be produced at these facilities will allow us to measure various flavor changing neutral current (FCNC) interactions. The quark level FCNC transition $b \to s(d)l^+l^-$, where $l = e, \mu, \tau$, are forbidden at the tree level in the SM and can occur only via one or more loops. Therefore, they have the potential to test higher order corrections to the SM and also to constrain many of its possible extensions. The quark level FCNC transitions $b \to s(d)l^+l^-$ give rise to the inclusive semileptonic decays $B \to X_s(X_d)l^+l^-$.

It is always good to consider new physics effects in the observables, which are either zero or highly suppressed in the SM. The reason is that any finite or large measurement of such an observable will confirm the existence of new physics. The *CP* asymmetry in $B \to (X_s, X_d)l^+l^-$ is one such observable. The *CP* asymmetry in $B \to (X_s, X_d)l^+l^-$ has been widely studied within the framework of the SM and its possible extensions [1–7]. In the SM, the *CP* asymmetry in $B \to X_s l^+l^-$ is $\sim 10^{-3}$ [1,2], whereas in $B \to X_d l^+l^-$ it is $\sim$(3–6)% [2–4]. In the SM with three generations (SM3), the only source of *CP* violation is the unique phase in the Cabibbo-Kobayashi-Maskawa (CKM) quark mixing matrix. However, in many possible extensions of the SM, there can be extra phases contributing to the *CP* asymmetry.

In this paper we study the *CP* asymmetry in $B \to (X_s, X_d)\mu^+\mu^-$ within the framework of the SM with an additional fourth generation (SM4). There is no clear theoretical argument to restrict the number of generations to three in the SM. Therefore, in principle we can have four or more generations. The effects of the extra generation have been studied in the literature in detail [8–18]. The existence of new-generation fermions that are lighter than $M_Z/2 \approx 45$ GeV has been excluded by the data on the width of the Z boson [19], whereas the existence of fermions heavier than $M_Z \approx 91$ GeV has been excluded by the existing data on the Z boson parameters combined with the masses of the W boson and the top quark [20]. However, using the same data one can show that a few extra generations are possible provided the neutral leptons have masses around 50 GeV [21,22].

The electroweak (EW) precision measurements impose severe constraints on the fourth generation [20,23–27]. A considerable amount of fine-tuning is required to accommodate a heavy fourth generation top quark t' ($m_{t'} > 400$ GeV) in order not to violate the experimental constraints from the S and T parameters [27]. The parameter space of fourth generation masses with minimal contributions to the EW precision oblique parameters, and in agreement with all experimental constraints, is [27]

$$\begin{aligned} m_{l'} - m_{\nu'} &\simeq (30\text{–}60)\ \text{GeV} \\ m_{t'} - m_{b'} &\simeq \left(1 + \frac{1}{5}\frac{m_H}{115\ \text{GeV}}\right) \times 50\ \text{GeV}, \end{aligned} \tag{1}$$

where m_H is the Higgs mass and $m_{l'}$, $m_{\nu'}$, $m_{b'}$ are the masses of the fourth generation charged lepton l', neutrino ν' and the down type quark b', respectively. We see that the EW precision data constrain the mass splitting between t' and b' (l' and ν') to be small, around 50 GeV.

The fourth generation has a significant effect on the Higgs sector of the SM. For example, the t' and b' quarks increase the effective ggH coupling by a factor of roughly 3, which will increase the production cross section $\sigma_{gg\to H}$ by almost an order of magnitude [28,29]. The effect of the

*alok@theory.tifr.res.in
†amol@theory.tifr.res.in
‡shamayitar@theory.tifr.res.in

fourth generation on Higgs physics has been studied in [27,30–32]. In [27], it was shown that in the SM4, Higgs masses between 115–315 (115–750) GeV are allowed by the EW precision data at the 68% (95%) C.L. Thus, the EW precision data favor a heavy Higgs boson if the fourth generation is introduced.

Rare decays of B mesons occur at loop level and hence they are sensitive to the generic extensions of the SM. The effects of the fourth generation on inclusive B decays have been studied in the literature [33–37]. We employ the Dighe-Kim parametrization [17] of the 4×4 quark mixing matrix (CKM4) that allows us to treat the effects of the fourth generation perturbatively and explore the complete parameter space available. We generalize the notion of unitarity triangles to unitarity quadrilaterals, and calculate the CP asymmetry.

The paper is organized as follows. In Sec. II, we present the theoretical expressions for the decay rate and CP asymmetry in $B \to (X_s, X_d)\mu^+\mu^-$. In Sec. III, we study constraints on the elements of CKM4, whereas in Secs. IV and V we present the estimates of CP asymmetry in $B \to X_s\mu^+\mu^-$ and $B \to X_d\mu^+\mu^-$, respectively. Finally in Sec. VI, we present our conclusions.

II. DECAY RATE AND CP ASYMMETRY IN $B \to (X_s, X_d)\mu^+\mu^-$

A. Effective Hamiltonian and decay rate

The effective Hamiltonian in the SM for the decay $b \to q\mu^+\mu^-$, where $q = s, d$, may be written as

$$H_{\rm eff} = \frac{4G_F}{\sqrt{2}} V_{tb}^* V_{tq} \sum_{i=1}^{10} C_i(\mu) O_i(\mu), \tag{2}$$

where the form of operators O_i and the expressions for calculating the coefficients $C_i(\mu)$ are given in [38]. The fourth generation only changes values of the Wilson coefficients $C_{7,8,9,10}$ via the virtual exchange of t'. The Wilson coefficients in the SM4 can be written as

$$C_i^{\rm tot}(\mu_b) = C_i(\mu_b) + \frac{V_{t'b}^* V_{t'q}}{V_{tb}^* V_{tq}} C_i^{t'}(\mu_b), \tag{3}$$

where $i = 7, 8, 9, 10$. The new Wilson coefficients $C_i^{t'}(\mu_b)$ can easily be calculated by substituting $m_{t'}$ for m_t in the SM3 expressions involving the t quark.

The amplitude for the decay $B \to X_q\mu^+\mu^-$ in the SM4 is given by

$$M = \frac{G_F\alpha}{\sqrt{2}\pi} V_{tb}^* V_{tq} \Big[C_9^{\rm tot} \bar{s}_L \gamma_\mu b_L \bar{\mu}\gamma^\mu \mu + C_{10}^{\rm tot} \bar{s}_L \gamma_\mu b_L \bar{\mu}\gamma^\mu\gamma^5 \mu + 2C_7^{\rm tot} m_b \bar{s}_L i\sigma_{\mu\nu} \frac{q^\mu}{q^2} b_R \bar{\mu}\gamma^\nu \mu \Big], \tag{4}$$

where the Wilson coefficients are evaluated at $\mu_b = m_b$. The calculation of the differential decay rate gives

$$\frac{dB(B \to X_q\mu^+\mu^-)}{dz} = \frac{\alpha^2 B(B \to X_c e\bar{\nu})}{4\pi^2 f(\hat{m}_c)\kappa(\hat{m}_c)} (1-z)^2 \times \left(1 - \frac{4t^2}{z}\right)^{1/2} \frac{|V_{tb}^* V_{tq}|^2}{|V_{cb}|^2} D(z), \tag{5}$$

where

$$D(z) = |C_9^{\rm tot}|^2 \left(1 + \frac{2t^2}{z}\right)(1+2z) + 4|C_7^{\rm tot}|^2 \left(1 + \frac{2t^2}{z}\right) \times \left(1 + \frac{2}{z}\right) + |C_{10}^{\rm tot}|^2 \left[(1+2z) + \frac{2t^2}{z}(1-4z)\right] + 12\,{\rm Re}(C_7^{\rm tot} C_9^{\rm tot*}) \left(1 + \frac{2t^2}{z}\right). \tag{6}$$

Here, $z \equiv q^2/m_b^2$, $t \equiv m_\mu/m_b$, and $\hat{m}_q = m_q/m_b$ for all quarks q. The phase space factor $f(\hat{m}_c)$ in $B(B \to X_c e\bar{\nu})$ is given by [39]

$$f(\hat{m}_c) = 1 - 8\hat{m}_c^2 + 8\hat{m}_c^6 - \hat{m}_c^8 - 24\hat{m}_c^4 \ln \hat{m}_c. \tag{7}$$

$\kappa(\hat{m}_c)$ is the 1-loop QCD correction factor [39]

$$\kappa(\hat{m}_c) = 1 - \frac{2\alpha_s(m_b)}{3\pi} \left[\left(\pi^2 - \frac{31}{4}\right)(1-\hat{m}_c)^2 + \frac{3}{2}\right]. \tag{8}$$

Within the SM3, the Wilson coefficients C_7 and C_{10} are real. However the Wilson coefficient C_9 becomes slightly complex due to the non-negligible terms induced by the continuum part of $u\bar{u}$ and $c\bar{c}$ loops proportional to $V_{ub}^* V_{uq}$ and $V_{cb}^* V_{cq}$, respectively. This complex nature of C_9 gives rise to the CP asymmetry in $B \to (X_s, X_d)\mu^+\mu^-$ in the SM3.

In the framework of the SM4, the Wilson coefficients $C_7^{\rm tot}$, $C_9^{\rm tot}$, and $C_{10}^{\rm tot}$ are given by

$$C_7^{\rm tot} = C_7(m_b) + \lambda_{tt'}^q C_7^{t'}(m_b), \tag{9}$$

$$C_9^{\rm tot} = \xi_1 + \lambda_{tu}^q \xi_2 + \lambda_{tt'}^q C_9^{t'}(m_b), \tag{10}$$

$$C_{10}^{\rm tot} = C_{10}(m_b) + \lambda_{tt'}^q C_{10}^{t'}(m_b), \tag{11}$$

where

$$\lambda_{tu}^q = \frac{\lambda_u^q}{\lambda_t^q} = \frac{V_{ub}^* V_{uq}}{V_{tb}^* V_{tq}}, \tag{12}$$

$$\lambda_{tt'}^q = \frac{\lambda_{t'}^q}{\lambda_t^q} = \frac{V_{t'b}^* V_{t'q}}{V_{tb}^* V_{tq}}, \tag{13}$$

so that all three relevant Wilson coefficients are complex in general. The parameters ξ_i are given by [38]

$$\xi_1 = C_9(m_b) + 0.138\omega(z) + g(\hat{m}_c, z)(3C_1 + C_2 + 3C_3 + C_4 + 3C_5 + C_6) - \tfrac{1}{2}g(\hat{m}_d, z)(C_3 + 3C_4) - \tfrac{1}{2}g(\hat{m}_b, z)(4C_3 + 4C_4 + 3C_5 + C_6) + \tfrac{2}{9}(3C_3 + C_4 + 3C_5 + C_6), \quad (14)$$

$$\xi_2 = [g(\hat{m}_c, z) - g(\hat{m}_u, z)](3C_1 + C_2). \quad (15)$$

Here,

$$\omega(z) = -\frac{2}{9}\pi^2 - \frac{4}{3}\mathrm{Li}_2(z) - \frac{2}{3}\ln z \ln(1-z) - \frac{5+4z}{3(1+2z)}\ln(1-z) - \frac{2z(1+z)(1-2z)}{3(1-z)^2(1+2z)}\ln z + \frac{5+9z-6z^2}{6(1-z)(1+2z)}, \quad (16)$$

with

$$\mathrm{Li}_2(z) = -\int_0^t dt \frac{\ln(1-t)}{t}. \quad (17)$$

The function $g(\hat{m}, z)$ represents the one loop corrections to the four-quark operators $O_1 - O_6$ and is given by [38]

$$g(\hat{m}, z) = -\frac{8}{9}\ln\frac{m_b}{\mu_b} - \frac{8}{9}\ln\hat{m} + \frac{8}{27} + \frac{4}{9}x - \frac{2}{9}(2+x)|1-x|^{1/2} \times \begin{cases} (\ln|\frac{\sqrt{1-x}+1}{\sqrt{1-x}-1}| - i\pi), & \text{for } x \equiv \frac{4\hat{m}^2}{z} < 1 \\ 2\arctan\frac{1}{\sqrt{x-1}}, & \text{for } x \equiv \frac{4\hat{m}^2}{z} > 1. \end{cases} \quad (18)$$

For light quarks, we have $\hat{m}_u \simeq \hat{m}_d \simeq 0$. In this limit,

$$g(0, z) = \frac{8}{27} - \frac{8}{9}\ln\frac{m_b}{\mu_b} - \frac{4}{9}\ln z + \frac{4}{9}i\pi. \quad (19)$$

We compute $g(\hat{m}, z)$ at $\mu_b = m_b$.

II. *CP* asymmetry in $B \to X_q \mu^+ \mu^-$

The *CP* asymmetry in $B \to X_q \mu^+ \mu^-$ is defined as

$$A_{CP}(z) = \frac{(dB/dz) - (d\overline{B}/dz)}{(dB/dz) + (d\overline{B}/dz)} = \frac{D(z) - \overline{D(z)}}{D(z) + \overline{D(z)}}, \quad (20)$$

where B and $\overline{B}$ represents the branching ratio of $\bar{B} \to X_q l^+ l^-$ and its complex conjugate $B \to \bar{X}_q l^+ l^-$, respectively. $d\overline{B}/dz$ can be obtained from dB/dz by making the following replacements:

$$C_7^{\mathrm{tot}} = C_7(m_b) + \lambda_{tt'}^q C_7^{t'}(m_b) \to \overline{C_7^{\mathrm{tot}}} = C_7(m_b) + \lambda_{tt'}^{q*} C_7^{t'}(m_b), \quad (21)$$

$$C_9^{\mathrm{tot}} = \xi_1 + \lambda_{tu}^q \xi_2 + \lambda_{tt'}^q C_9^{t'}(m_b) \to \overline{C_9^{\mathrm{tot}}} = \xi_1 + \lambda_{tu}^{q*} \xi_2 + \lambda_{tt'}^{q*} C_9^{t'}(m_b), \quad (22)$$

$$C_{10}^{\mathrm{tot}} = C_{10}(m_b) + \lambda_{tt'}^q C_{10}^{t'}(m_b) \to \overline{C_{10}^{\mathrm{tot}}} = C_{10}(m_b) + \lambda_{tt'}^{q*} C_{10}^{t'}(m_b). \quad (23)$$

Then

$$D(z) - \overline{D(z)} = 2\left(1 + \frac{2t^2}{z}\right)[\mathrm{Im}(\lambda_{tu}^q)\{2(1+2z)\,\mathrm{Im}(\xi_1\xi_2^*) - 12C_7\,\mathrm{Im}(\xi_2)\} + X_{\mathrm{im}}\{(1+2z)C_9^{t'} + 6C_7^{t'}\}], \quad (24)$$

$$D(z) + \overline{D(z)} = \left(1 + \frac{2t^2}{z}\right)[(1+2z)\{B_1 + 2C_9^{t'}(|\lambda_{tt'}^q|^2 C_9^{t'} + X_{\mathrm{re}})\} + 12\{B_2 + 2C_7 C_9^{t'}\,\mathrm{Re}(\lambda_{tt'}^q) + C_7^{t'}(2|\lambda_{tt'}^q|^2 C_9^{t'} + X_{\mathrm{re}})\}] + 8\left(1 + \frac{2t^2}{z}\right) \times \left(1 + \frac{2}{z}\right)|C_7^{\mathrm{tot}}|^2 + 2\left[(1+2z) + \frac{2t^2}{z}(1-4z)\right] \times |C_{10}^{\mathrm{tot}}|^2, \quad (25)$$

where

$$X_{\mathrm{re}} = 2\{\mathrm{Re}(\lambda_{tt'}^q)\,\mathrm{Re}(\xi_1) + \mathrm{Re}(\lambda_{tt'}^q \lambda_{tu}^{q*})\,\mathrm{Re}(\xi_2)\}, \quad (26)$$

$$X_{\mathrm{im}} = 2\{\mathrm{Im}(\lambda_{tt'}^q)\,\mathrm{Im}(\xi_1) + \mathrm{Im}(\lambda_{tt'}^q \lambda_{tu}^{q*})\,\mathrm{Im}(\xi_2)\}, \quad (27)$$

$$B_1 = 2\{|\xi_1|^2 + |\lambda_{tu}^q \xi_2|^2 + 2\,\mathrm{Re}(\lambda_{tu}^q)\,\mathrm{Re}(\xi_1\xi_2^*)\}, \quad (28)$$

$$B_2 = 2C_7\{\mathrm{Re}(\xi_1) + \mathrm{Re}(\lambda_{tu}^q)\,\mathrm{Re}(\xi_2)\}, \quad (29)$$

$$|C_{10}^{\mathrm{tot}}|^2 = (C_{10})^2 + |\lambda_{tt'}^q|^2 (C_{10}^{t'})^2 + 2C_{10}C_{10}^{t'}\,\mathrm{Re}(\lambda_{tt'}^q), \quad (30)$$

$$|C_7^{\mathrm{tot}}|^2 = (C_7)^2 + |\lambda_{tt'}^q|^2 (C_7^{t'})^2 + 2C_7 C_7^{t'}\,\mathrm{Re}(\lambda_{tt'}^q). \quad (31)$$

The theoretical calculations shown above for the branching ratio of $B \to X_q \mu^+ \mu^-$ are rather uncertain in the intermediate q^2 region ($7\ \mathrm{GeV}^2 < q^2 < 12\ \mathrm{GeV}^2$) owing to the vicinity of charmed resonances. The predictions are relatively more robust in the lower and higher q^2 regions. We therefore concentrate on calculating $A_{CP}(q^2)$ in the low-q^2 ($1\ \mathrm{GeV}^2 < q^2 < 6\ \mathrm{GeV}^2$) and the high-$q^2$ ($14.4\ \mathrm{GeV}^2 < q^2 < m_b^2$) regions. In terms of the dimensionless parameter $z = q^2/m_b^2$, the low-q^2 region corresponds to $0.043 < z < 0.26$, whereas the high q^2 region corresponds to $0.62 < z < 1$.

In order to estimate A_{CP}, we need to know the magnitude and phase of λ_{tu}^q and $\lambda_{tt'}^q$. For this we use the Dighe-Kim (DK) parametrization of the CKM4 matrix elements, introduced in [17].

III. THE QUARK MIXING MATRIX IN SM4

DK parametrization for the 4×4 matrix CKM4

The CKM matrix in the SM is a 3×3 unitary matrix represented as

$$V_{\mathrm{CKM3}} = \begin{pmatrix} V_{ud} & V_{us} & V_{ub} \\ V_{cd} & V_{cs} & V_{cb} \\ V_{td} & V_{ts} & V_{tb} \end{pmatrix}. \tag{32}$$

In the SM4, a general CKM matrix can be written as follows:

$$V_{\mathrm{CKM4}} = \begin{pmatrix} \tilde{V}_{ud} & \tilde{V}_{us} & \tilde{V}_{ub} & \tilde{V}_{ub'} \\ \tilde{V}_{cd} & \tilde{V}_{cs} & \tilde{V}_{cb} & \tilde{V}_{cb'} \\ \tilde{V}_{td} & \tilde{V}_{ts} & \tilde{V}_{tb} & \tilde{V}_{tb'} \\ \tilde{V}_{t'd} & \tilde{V}_{t's} & \tilde{V}_{t'b} & \tilde{V}_{t'b'} \end{pmatrix}. \tag{33}$$

The above matrix can be described, with appropriate choices for the quark phases, in terms of 6 real quantities and 3 phases. The DK parametrization defines

$$\tilde{V}_{us} \equiv \lambda, \qquad \tilde{V}_{cb} \equiv A\lambda^2, \qquad \tilde{V}_{ub} \equiv A\lambda^3 C e^{-i\delta_{ub}},$$
$$\tilde{V}_{ub'} \equiv p\lambda^3 e^{-i\delta_{ub'}}, \qquad \tilde{V}_{cb'} \equiv q\lambda^2 e^{-i\delta_{cb'}}, \qquad \tilde{V}_{tb'} \equiv r\lambda. \tag{34}$$

The CKM4 matrix now looks like

$$V_{\mathrm{CKM4}} = \begin{pmatrix} \# & \lambda & A\lambda^3 C e^{-i\delta_{ub}} & p\lambda^3 e^{-i\delta_{ub'}} \\ \# & \# & A\lambda^2 & q\lambda^2 e^{-i\delta_{cb'}} \\ \# & \# & \# & r\lambda \\ \# & \# & \# & \# \end{pmatrix}. \tag{35}$$

The elements denoted by "#" can be determined uniquely from the unitarity condition $V^{\dagger}_{\mathrm{CKM4}} V_{\mathrm{CKM4}} = I$ on CKM4. They can be calculated in the form of an expansion in the powers of λ such that each element is accurate up to a multiplicative factor of $[1 + \mathcal{O}(\lambda^3)]$. The matrix elements $\tilde{V}_{ud}$, $\tilde{V}_{cd}$, and $\tilde{V}_{cs}$ retain their SM3 values

$$\tilde{V}_{ud} = 1 - \frac{\lambda^2}{2} + \mathcal{O}(\lambda^4), \tag{36}$$

$$\tilde{V}_{cd} = -\lambda + \mathcal{O}(\lambda^5), \tag{37}$$

$$\tilde{V}_{cs} = 1 - \frac{\lambda^2}{2} + \mathcal{O}(\lambda^4), \tag{38}$$

whereas the values of the matrix elements V_{td}, V_{ts}, and V_{tb} are modified due to the presence of the additional quark generation:

$$\tilde{V}_{td} = A\lambda^3(1 - Ce^{i\delta_{ub}}) + r\lambda^4(qe^{i\delta_{cb'}} - pe^{i\delta_{ub'}}) + \frac{A}{2}\lambda^5(-r^2 + (C + Cr^2)e^{i\delta_{ub}}) + \mathcal{O}(\lambda^6), \tag{39}$$

$$\tilde{V}_{ts} = -A\lambda^2 - qr\lambda^3 e^{i\delta_{cb'}} + \frac{A}{2}\lambda^4(1 + r^2 - 2Ce^{i\delta_{ub}}) + \mathcal{O}(\lambda^5), \tag{40}$$

$$\tilde{V}_{tb} = 1 - \frac{r^2\lambda^2}{2} + \mathcal{O}(\lambda^4). \tag{41}$$

In the limit $p = q = r = 0$, only the elements present in the 3×3 CKM matrix retain nontrivial values, and the above expansion corresponds to the Wolfenstein parametrization [40] with $C = \sqrt{\rho^2 + \eta^2}$ and $\delta_{ub} = \tan^{-1}(\eta/\rho)$. The remaining new CKM4 matrix elements are

$$\tilde{V}_{t'd} = \lambda^3(qe^{i\delta_{cb'}} - pe^{i\delta_{ub'}}) + Ar\lambda^4(1 + Ce^{i\delta_{ub}}) + \frac{\lambda^5}{2}(pe^{i\delta_{ub'}} - qr^2 e^{i\delta_{cb'}} + pr^2 e^{i\delta_{ub'}}) + \mathcal{O}(\lambda^6), \tag{42}$$

$$\tilde{V}_{t's} = q\lambda^2 e^{i\delta_{cb'}} + Ar\lambda^3 + \lambda^4\left(-pe^{i\delta_{ub'}} + \frac{q}{2}e^{i\delta_{cb'}} + \frac{qr^2}{2}e^{i\delta_{cb'}}\right) + \mathcal{O}(\lambda^5), \tag{43}$$

$$\tilde{V}_{t'b} = -r\lambda + \mathcal{O}(\lambda^4), \tag{44}$$

$$\tilde{V}_{t'b'} = 1 - \frac{r^2\lambda^2}{2} + \mathcal{O}(\lambda^4). \tag{45}$$

We already have strong direct bounds on the magnitudes of the elements of the CKM3 matrix. From the direct measurements of $|\tilde{V}_{us}| = |V_{us}|$, $|\tilde{V}_{cb}| = |V_{cb}|$, and $|\tilde{V}_{ub}/\tilde{V}_{cb}| = |V_{ub}/V_{cb}|$ [19], which do not assume the unitarity of the CKM matrix, one can derive [17]

$$0.216 < \lambda < 0.223, \qquad 0.76 < A < 0.90, \qquad 0.23 < C < 0.59 \tag{46}$$

at 90% C.L. Also, the phase δ_{ub} can be constrained through the measurement of $\gamma \equiv \mathrm{Arg}(-V^*_{ub}V_{ud})/(V^*_{cb}V_{cd})$ since from (34), (36), and (37),

$$\mathrm{Arg}\left(-\frac{V^*_{ub}V_{ud}}{V^*_{cb}V_{cd}}\right) \approx \mathrm{Arg}\left(-\frac{\tilde{V}^*_{ub}\tilde{V}_{ud}}{\tilde{V}^*_{cb}\tilde{V}_{cd}}\right) \approx \delta_{ub}. \tag{47}$$

The value of δ_{ub} is therefore restricted to lie between (26°–125°) at 90% C.L.

Direct bounds on p and q can be obtained by combining the direct measurements of the magnitudes of the elements in the first two rows with the unitarity constraints. We get the 90% C.L. bounds on $|\tilde{V}_{ub'}|$ and $|\tilde{V}_{cb'}|$ as

$$|\tilde{V}_{ub'}| < 0.094, \qquad |\tilde{V}_{cb'}| < 0.147, \tag{48}$$

which correspond to $p < 9.0$, $q < 3.05$. In addition, a strong constraint is obtained on the combination $X^L_{bb} \equiv (V^{\dagger}_{\mathrm{CKM4}}V_{\mathrm{CKM4}})_{bb}$ through the measurements involving $Z \to b\bar{b}$, which give $X^L_{bb} = 0.996 \pm 0.005$ [41]. This translates to $|\tilde{V}_{t'b}| < 0.11$ at 90% C.L., which corresponds to $r < 0.5$.

The observables ΔM_{B_s}, ΔM_{B_d}, $B \to X_s\gamma$, $B \to X_s\mu^+\mu^-$, and $\sin 2\beta$ are complicated functions of the CKM parameters λ, A, C, p, q, r, $\delta_{ub'}$, δ_{ub}, and $\delta_{cb'}$. Hence, we take care of the constraints on these parameters numerically, without giving the analytic expressions explicitly here.

IV. *CP* ASYMMETRY IN $B \to X_s\mu^+\mu^-$

A. Unitarity quadrilateral relevant for $B \to X_s\mu^+\mu^-$

The "squashed" unitarity triangle in the SM3 that arises from the equation

$$V_{cb}^* V_{cs} + V_{ub}^* V_{us} + V_{tb}^* V_{ts} = 0 \tag{49}$$

is shown in Fig. 1. The angles of this unitarity triangle are

$$\begin{aligned} \chi &\equiv \mathrm{Arg}\left(-\frac{V_{cb}^* V_{cs}}{V_{tb}^* V_{ts}}\right), \\ \Theta &\equiv \mathrm{Arg}\left(-\frac{V_{tb}^* V_{ts}}{V_{ub}^* V_{us}}\right) = \gamma - \chi, \qquad \pi - \Theta - \chi. \end{aligned} \tag{50}$$

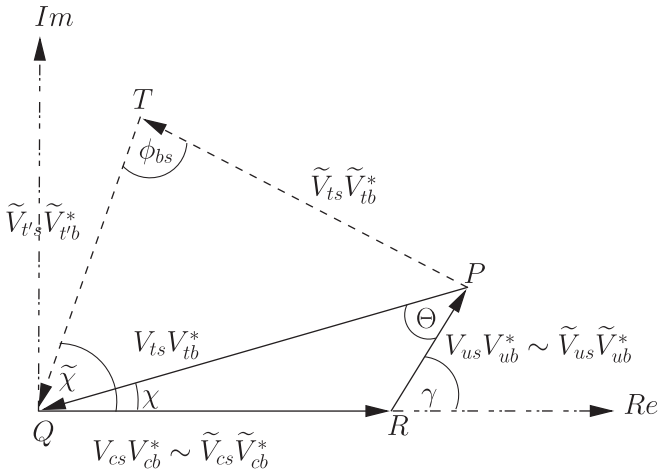

FIG. 1. The "squashed" unitarity triangle (PQR) in the SM3 and the corresponding unitarity quadrilateral (QRPT) in the SM4.

The corresponding unitarity "quadrilateral" relation in the SM4 is

$$\tilde{V}_{cb}^* \tilde{V}_{cs} + \tilde{V}_{ub}^* \tilde{V}_{us} + \tilde{V}_{tb}^* \tilde{V}_{ts} + \tilde{V}_{t'b}^* \tilde{V}_{t's} = 0. \tag{51}$$

This quadrilateral may be superimposed on the SM unitarity triangle as shown in Fig. 1.

The *CP* asymmetry in the SM3 depends on $\mathrm{Im}(\lambda_{tu}^s)$, as can be seen from Eq. (24). This quantity may be written as

$$\mathrm{Im}\,(\lambda_{tu}^s) = -C\lambda^2 \sin\delta_{ub} + \mathcal{O}(\lambda^3), \tag{52}$$

which is the same as the sine of the angle χ shown in Fig. 1. With the introduction of the fourth generation, the contribution to the *CP* asymmetry also comes from the quantity $\mathrm{Im}(\lambda_{tt'}^s)$, which may be written as

$$\mathrm{Im}\,(\lambda_{tt'}^s) = \frac{qr\sin\delta_{cb'}}{A}\lambda + \mathcal{O}(\lambda^2), \tag{53}$$

which is the same as the sine of the angle $\tilde{\chi}$ in the figure. Thus, the new CKM4 elements themselves tend to magnify the *CP* violation by a factor of $\sim 1/\lambda \approx 5$. There can of course be additional factors due to the modified Wilson coefficients in SM4, which we will take care of in our complete numerical analysis in the next section.

B. Numerical calculation of $A_{CP}(q^2)$ in $B \to X_s\mu^+\mu^-$

In order to calculate $A_{CP}(q^2)$ from the procedure outlined in Sec. II B, we need to know λ_{tu}^q and $\lambda_{tt'}^q$. Using the DK parametrization, we have

$$\lambda_{tt'}^s = \frac{e^{i\delta_{cb'}} qr\lambda}{A} + \left(r - \frac{e^{2i\delta_{cb'}} q^2 r^2}{A^2}\right)\lambda^2 + \mathcal{O}(\lambda^3), \tag{54}$$

$$\lambda_{tu}^s = -Ce^{i\delta_{ub}}\lambda^2 + \mathcal{O}(\lambda^3). \tag{55}$$

Putting these values of λ_{tu}^s and $\lambda_{tt'}^s$ in the relevant expressions in Sec. II B, we obtain $A_{CP}(q^2)$ in $B \to X_s\mu^+\mu^-$. The inputs used in the numerical analysis are shown in Table I.

Figure 2 shows $A_{CP}(q^2)$ in the low and high q^2 regions for the decay $B \to X_s\mu^+\mu^-$ for $m_{t'} = (400, 800, 1200)$ GeV. Clearly for $m_{t'} = 400$ GeV, for

TABLE I. Numerical inputs used in our analysis. Unless explicitly specified, they are taken from the Review of Particle Physics [19].

$G_F = 1.166 \times 10^{-5}$ GeV^{-2}	$m_c/m_b = 0.29$	[42]
$\alpha = 1.0/129.0$	$f_{B_s}\sqrt{\hat{B}_s} = (0.270 \pm 0.030)$ GeV	[43]
$\alpha_s(m_b) = 0.220$ [44]	$f_{B_d}\sqrt{\hat{B}_d} = (0.225 \pm 0.025)$ GeV [43]	
$\tau_{B_s} = 1.45 \times 10^{-12}$ s	$m_s = (1.17 \pm 0.008) \times 10^{-11}$ GeV	
$\tau_{B_d} = 1.53 \times 10^{-12}$ s	$\Delta m_d = (3.337 \pm 0.033) \times 10^{-13}$ GeV	
$m_\mu = 0.105$ GeV	$\sin 2\beta = 0.681 \pm 0.025$	
$m_W = 80.40$ GeV	$\delta_{ub}(\equiv \gamma) = (77^{+30}_{-32})^\circ$	
$m_t = 172.5$ GeV	$B(B \to X_c\ell\nu) = 0.1061 \pm 0.0016 \pm 0.0006$ [45]	
$m_b = 4.80$ GeV [42]	$B(B \to X_s\mu^+\mu^-)_{q^2>14.4\ \mathrm{GeV}} = (0.44 \pm 0.12) \times 10^{-6}$ [46,47]	
$m_{B_s} = 5.366$ GeV	$B(B \to X_s\gamma) = (3.55 \pm 0.25) \times 10^{-4}$ [48]	
$m_B = 5.279$ GeV		

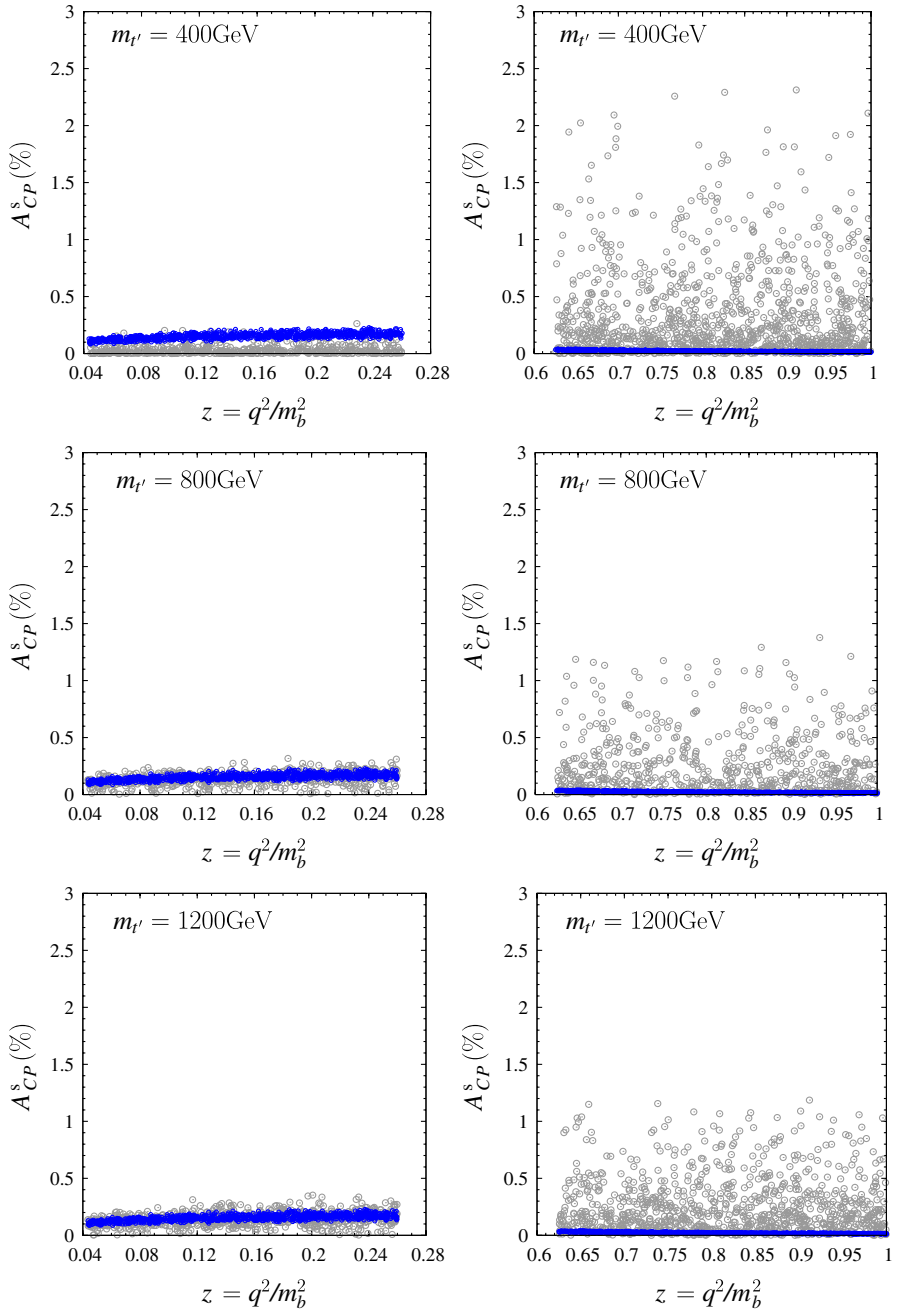

FIG. 2 (color online). $A_{CP}(z)$ vs z plot in the low-q^2 (left panel) and the high-q^2 (right panel) regions for the decay $B \to X_s \mu^+ \mu^-$ for $m_{t'} = (400, 800, 1200)$ GeV. The blue band represents the SM3 prediction, whereas the grey circles correspond to the possible values that can be obtained in the SM4.

most of the allowed regions of the parameter space, the SM4 prediction for $A_{CP}(q^2)$ in the low-q^2 region is either below the SM3 prediction or consistent with it. However, in the high-q^2 region, the SM4 prediction can be as high as 2.5%, which is about 40 times the SM3 prediction. There is thus a significant enhancement in $A_{CP}(q^2)$ in the high-q^2 region.

Table II shows the ratio of the maximum $A_{CP}(q^2)$ allowed within the SM4 and that allowed in the SM3. It can be seen that with increasing $m_{t'}$, the enhancement in $A_{CP}(q^2)$ at low q^2 (high q^2) increases (decreases) and then saturates at $\sim$1.2 (25) times the SM value. Thus, while the low-q^2 region is rather insensitive to the effects of the fourth generation, the high-q^2 region may show a significant asymmetry that can easily be shown to be beyond the limits of the SM3.

The saturation in $A_{CP}(q^2)$ at large $m_{t'}$ may be understood as follows. The Wilson coefficient C_{10} becomes very large as compared to C_7 and C_9 for large $m_{t'}$. Hence, from Eq. (11), it is obvious that $\lambda^s_{tt'}$ must be very small for large $m_{t'}$

TABLE II. Comparison of $A_{CP}(q^2)$ in the SM3 and in the SM4 for $B \to X_s \mu^+ \mu^-$ at different $m_{t'}$ values.

	$[A^s_{CP}(q^2)]_{\max}$ (low q^2)			$[A^s_{CP}(q^2)]_{\max}$ (high q^2)		
$m_{t'}$ (GeV)	SM3	SM4	SM4/SM3	SM3	SM4	SM4/SM3
400	0.25%	0.25%	1.0	0.05%	2.3%	46
800	0.25%	0.3%	1.2	0.05%	1.4%	28
1200	0.25%	0.3%	1.2	0.05%	1.3%	26

so as to keep the branching ratio within the experimental range. Hence, in the limit of large $m_{t'}$, we have $\lambda^s_{tt'} \to 0$. In this limit, the $X_{\rm im}$ term in Eq. (24) vanishes and the numerator of $A_{CP}(q^2)$ becomes

$$D(z) - \overline{D(z)} = 2\left(1 + \frac{2t^2}{z}\right)[\mathrm{Im}(\lambda^q_{tu})\{2(1+2z)\,\mathrm{Im}(\xi_1 \xi_2^*) - 12 C_7\,\mathrm{Im}(\xi_2)\}]. \tag{56}$$

The right-hand side of Eq. (56) has only a weak dependence on $m_{t'}$ and hence remains almost constant for large $m_{t'}$. $D(z) + \overline{D(z)}$, on the other hand, is just obtained from the branching ratio of $B \to X_s \mu^+ \mu^-$, an experimentally measured value. The ratio of these two quantities, $A_{CP}(q^2)$, is therefore rather independent of $m_{t'}$ at large $m_{t'}$. This fact is reflected in the A_{CP} plots: there is not much difference in the $A_{CP}(q^2)$ prediction for $m_{t'} = 800$ GeV and $m_{t'} = 1200$ GeV.

V. *CP* ASYMMETRY IN $B \to X_d \mu^+ \mu^-$

A. Unitarity quadrilateral relevant for $B \to X_d \mu^+ \mu^-$

The "standard" unitarity triangle in the SM3, which arises from the equation

$$V^*_{ub} V_{ud} + V^*_{cb} V_{cd} + V^*_{tb} V_{td} = 0 \tag{57}$$

is shown in Fig. 3 The angles of this unitarity triangle are defined as

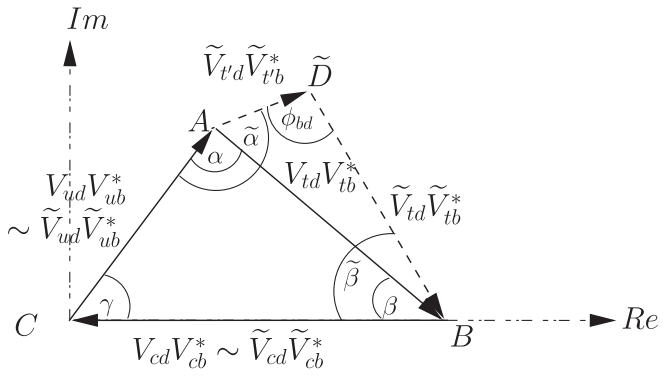

FIG. 3. The unitarity triangle (ABC) in the SM3 and the corresponding unitarity quadrilateral (ACBD) in the SM4.

$$\alpha \equiv \mathrm{Arg}\left(-\frac{V^*_{tb}V_{td}}{V^*_{ub}V_{ud}}\right), \qquad \beta \equiv \mathrm{Arg}\left(-\frac{V^*_{cb}V_{cd}}{V^*_{tb}V_{td}}\right), \qquad \gamma \equiv \mathrm{Arg}\left(-\frac{V^*_{ub}V_{ud}}{V^*_{cb}V_{cd}}\right). \tag{58}$$

The corresponding unitarity relation in the SM4 is

$$\tilde{V}^*_{ub}\tilde{V}_{ud} + \tilde{V}^*_{cb}\tilde{V}_{cd} + \tilde{V}^*_{tb}\tilde{V}_{td} + \tilde{V}^*_{t'b}\tilde{V}_{t'd} = 0. \tag{59}$$

This quadrilateral may be superimposed on the SM unitarity triangle as shown in Fig. 3.

The *CP* asymmetry in SM3 depends on $\mathrm{Im}(\lambda^d_{tu})$, as can be seen from Eq. (24). This quantity may be written as

$$\mathrm{Im}\,(\lambda^d_{tu}) = -\mathrm{Arg}\left(\frac{e^{i\delta_{ub}}}{1 - Ce^{i\delta_{ub}}}\right) + \mathcal{O}(\lambda), \tag{60}$$

which is the same as the sine of the angle β shown in Fig. 3. With the introduction of the fourth generation, contribution to the *CP* asymmetry also comes from the quantity $\mathrm{Im}(\lambda^d_{tt'})$, which may be written as

$$\mathrm{Im}\,(\lambda^d_{tt'}) = \mathcal{O}(\lambda). \tag{61}$$

Thus, the additional contribution to the *CP* violation from the complex nature of the CKM4 elements is rather small. The enhancement in $A_{CP}(q^2)$, if any, therefore has to come from the modified values of the Wilson coefficients. We calculate the enhancement numerically in the next section.

B. Numerical calculation of $A_{CP}(q^2)$ in $B \to X_d \mu^+ \mu^-$

We now consider λ^d_{tu} and $\lambda^d_{tt'}$ for the calculation of $A_{CP}(q^2)$ in $B \to X_d \mu^+ \mu^-$ using the procedure outlined in Sec. II B. Using the DK parametrization, we obtain

$$\lambda^d_{tt'} = \frac{(pe^{i\delta_{ub'}} - qe^{i\delta_{cb'}})r\lambda}{A(1 - Ce^{i\delta_{ub}})} + \mathcal{O}(\lambda^2), \tag{62}$$

$$\lambda^d_{tu} = \frac{e^{i\delta_{ub}}}{1 - Ce^{i\delta_{ub}}} + \frac{e^{i\delta_{ub}}(pe^{i\delta_{ub'}} - qe^{i\delta_{cb'}})r\lambda}{A(1 - Ce^{i\delta_{ub}})^2} + \mathcal{O}(\lambda^2). \tag{63}$$

For our numerical analysis, we use the expressions correct up to $\mathcal{O}(\lambda^2)$.

Figure 4 shows the $A_{CP}(q^2)$ distribution in the low-q^2 and the high-q^2 regions for $m_{t'} = (400, 800, 1200)$ GeV. Here, we find that for $m_{t'} = 400$ GeV, the low-q^2 prediction in the SM4 is either consistent with or below the SM3

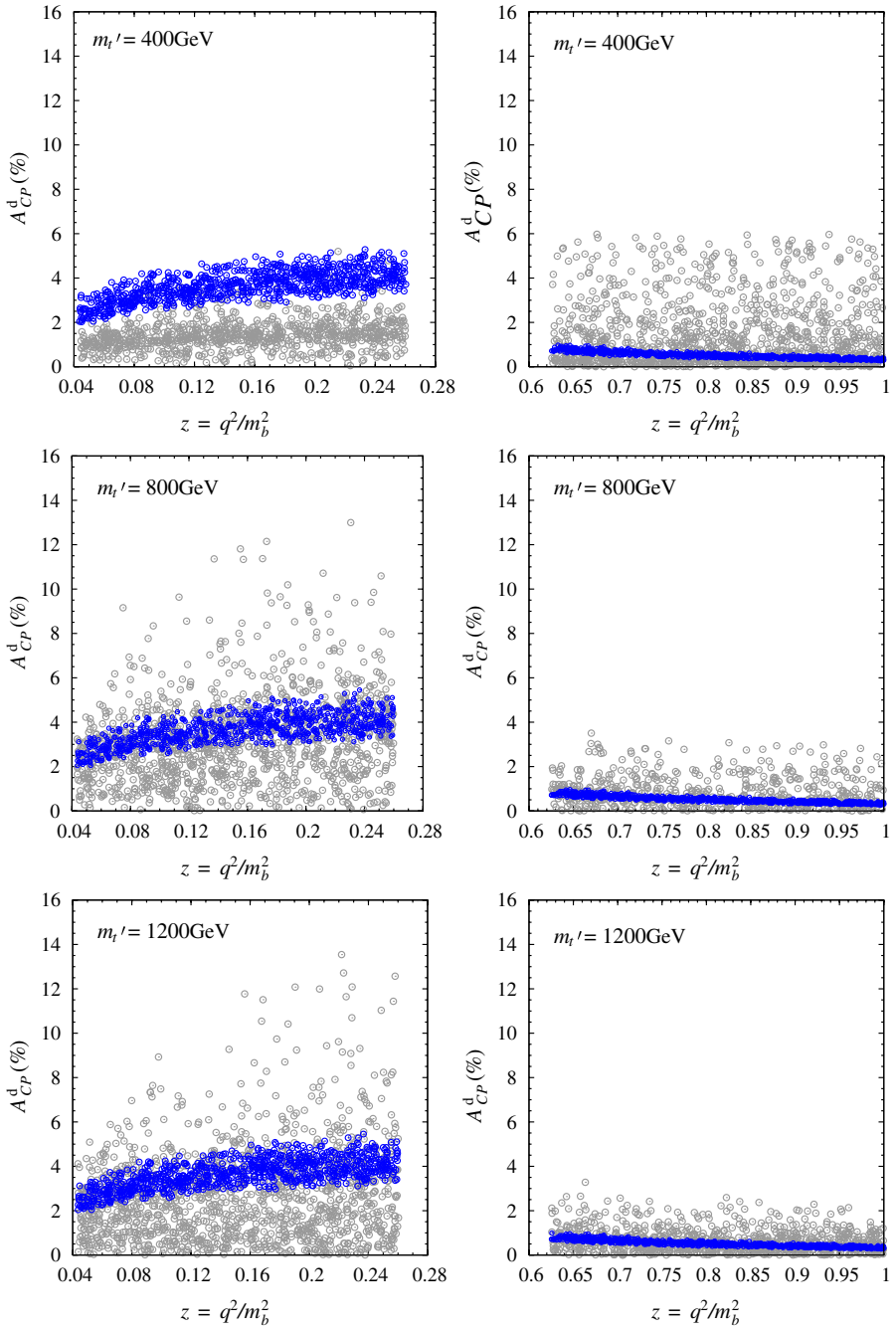

FIG. 4 (color online). $A_{CP}(z)$ vs z plot in (a) the low-q^2 and (b) the high-q^2 region for the decay $B \to X_d \mu^+ \mu^-$ for $m_{t'} = (400, 800, 1200)$ GeV.

prediction, whereas in the high-q^2 region, the SM4 prediction can be as high as 6%, which is about 6 times the SM3 prediction. There is thus a significant enhancement in $A_{CP}(q^2)$ in the high-q^2 region.

Table III shows the ratio of the maximal values of $A_{CP}(q^2)$ allowed within the SM4 and that allowed in the SM3. It can be seen that with increasing $m_{t'}$, the enhancement in $A_{CP}(q^2)$ at low-q^2 (high q^2) increases (decreases) and then saturates at $\sim$2.5 (3) times the SM3 value. At low $m_{t'}$, the enhancement in the high-q^2 region is rather large,

TABLE III. Comparison of $A_{CP}(q^2)$ in the SM3 and in the SM4 for $B \to X_d \mu^+ \mu^-$ at different $m_{t'}$ values.

	$[A^s_{CP}(q^2)]_{\max}$ (low q^2)			$[A^s_{CP}(q^2)]_{\max}$ (high q^2)		
$m_{t'}$ (GeV)	SM3	SM4	SM4/SM3	SM3	SM4	SM4/SM3
400	5.5%	5.5%	1.0	1.0%	6.0%	6.0
800	5.5%	13.5%	2.45	1.0%	4.0%	4.0
1200	5.5%	13.5%	2.45	1.0%	3.0%	3.0

and makes this region more suitable for the detection of a deviation from the SM3 expectation, just like in the case of $B \to X_s \mu^+ \mu^-$. However, at high $m_{t'}$, the enhancement over the SM3 value is similar in both the regions, so that the higher branching ratio at low q^2 and the higher value of $A_{CP}(q^2)$ therein makes the analysis of $B \to X_d \mu^+ \mu^-$ at low q^2 an interesting prospect.

The same arguments as given in Sec. IV B in the case of $B \to X_s \mu^+ \mu^-$ for the saturation of $A_{CP}(q^2)$ at large $m_{t'}$ also apply to $B \to X_d \mu^+ \mu^-$. The allowed range $A_{CP}(q^2)$ at 800 GeV and 1200 GeV is then almost identical, as can be seen in Fig. 4.

VI. CONCLUSIONS

In this paper we study the *CP* asymmetry in the decays $B \to X_s \mu^+ \mu^-$ and $B \to X_d \mu^+ \mu^-$ in the standard model with an additional fourth generation using the Dighe-Kim parametrization, which allows us to treat the problem as a perturbative expansion in the Cabibbo angle λ, and explore the complete parameter space of the 4×4 quark mixing matrix. We use constraints from the present measurements of ΔM_{B_s}, ΔM_{B_d}, $\sin 2\beta$, and the branching ratios of $B \to X_c e \bar{\nu}$, $B \to X_s \gamma$, $B \to X_s \mu^+ \mu^-$. The results may be summarized as follows:

(1) For the decay $B \to X_s \mu^+ \mu^-$, the fourth generation of quarks may provide more than an order of magnitude enhancement in $A_{CP}(q^2)$ in the high-q^2 region (for $m_{t'} > 400$ GeV), whereas practically no enhancement in the low-q^2 region is obtained. Therefore, the high-q^2 region is more sensitive to new physics of this kind.

(2) For the decay $B \to X_d \mu^+ \mu^-$, the fourth generation of quarks may provide an enhancement up to 6 times in $A_{CP}(q^2)$ in the high-q^2 region. While no enhancement is possible in the low-q^2 region for $m_{t'}$ around 400 GeV, at large $m_{t'}$ (> 800 GeV) the enhancement in both the low- and high-q^2 region in the SM4 is about 3 times the corresponding SM3 prediction. Since the branching ratio in the high-q^2 region is small compared to the one in the low-q^2 region, the low-q^2 region becomes more attractive at large $m_{t'}$.

(3) For both the decays $B \to (X_s, X_d) \mu^+ \mu^-$, the effect of increasing $m_{t'}$ is to increase (decrease) the values of $A_{CP}(q^2)$ in the low-q^2 (high-q^2) region. At large $m_{t'}$, the value of $A_{CP}(q^2)$ is almost independent of $m_{t'}$.

For a branching ratio of $\sim 10^{-6}$, a measurement of a *CP* asymmetry of 1% at the 3σ level would require $\sim 10^{10}$ B mesons. Hence, the measurement of a *CP* asymmetry at the level of a few percent should be feasible at the future colliders like super-*B* factories [49,50]. Any enhancement observed beyond the standard model, combined with its q^2 dependence, can offer clues about the nature of new physics involved.

ACKNOWLEDGMENTS

A. D. would like to thank C. S. Kim for useful discussions.

[1] D. S. Du and M. Z. Yang, Phys. Rev. D **54**, 882 (1996).
[2] A. Ali and G. Hiller, Eur. Phys. J. C **8**, 619 (1999).
[3] F. Kruger and L. M. Sehgal, Phys. Rev. D **55**, 2799 (1997).
[4] Z. D. Eygi and G. Turan, Mod. Phys. Lett. A **18**, 2735 (2003).
[5] L. T. Handoko, Phys. Rev. D **57**, 1776 (1998).
[6] S. Fukae, Phys. Rev. D **64**, 054010 (2001).
[7] V. Bashiry, J. Phys. G **32**, 1073 (2006).
[8] D. London, Phys. Lett. B **234**, 354 (1990).
[9] W. S. Hou and R. G. Stuart, Nucl. Phys.**B349**, 91 (1991).
[10] P. Bamert and C. P. Burgess, Z. Phys. C **66**, 495 (1995).
[11] T. Inami, T. Kawakami, and C. S. Lim, Mod. Phys. Lett. A **10**, 1471 (1995).
[12] A. Masiero, F. Feruglio, S. Rigolin, and R. Strocchi, Phys. Lett. B **355**, 329 (1995).
[13] V. A. Novikov, L. B. Okun, A. N. Rozanov, and M. I. Vysotsky, Rep. Prog. Phys. **62**, 1275 (1999).
[14] J. Erler and P. Langacker, Eur. Phys. J. C **3**, 90 (1998).
[15] W. S. Hou, M. Nagashima, and A. Soddu, Phys. Rev. Lett. **95**, 141601 (2005).
[16] W. S. Hou, H. n. Li, S. Mishima, and M. Nagashima, Phys. Rev. Lett. **98**, 131801 (2007).
[17] C. S. Kim and A. S. Dighe, Int. J. Mod. Phys. E **16**, 1445 (2007).
[18] A. Soni, A. K. Alok, A. Giri, R. Mohanta, and S. Nandi, arXiv:0807.1971.
[19] C. Amsler *et al.* (Particle Data Group), Phys. Lett. B **667**, 1 (2008).
[20] M. Maltoni, V. A. Novikov, L. B. Okun, A. N. Rozanov, and M. I. Vysotsky, Phys. Lett. B **476**, 107 (2000).
[21] P. H. Frampton, P. Q. Hung, and M. Sher, Phys. Rep. **330**, 263 (2000).
[22] J. I. Silva-Marcos, J. High Energy Phys. 12 (2002) 036.
[23] V. A. Novikov, L. B. Okun, A. N. Rozanov, M. I. Vysotsky, and V. P. Yurov, Mod. Phys. Lett. A **10**, 1915 (1995); **11**, 687 (1996).
[24] N. J. Evans, Phys. Lett. B **340**, 81 (1994).
[25] H. J. He, N. Polonsky, and S. f. Su, Phys. Rev. D **64**, 053004 (2001).
[26] V. A. Novikov, L. B. Okun, A. N. Rozanov, and M. I. Vysotsky, Phys. Lett. B **529**, 111 (2002).
[27] G. D. Kribs, T. Plehn, M. Spannowsky, and T. M. P. Tait, Phys. Rev. D **76**, 075016 (2007).
[28] J. F. Gunion, D. W. McKay, and H. Pois, Phys. Lett. B **334**,

339 (1994).
[29] J. F. Gunion, D. W. McKay, and H. Pois, Phys. Rev. D **53**, 1616 (1996).
[30] E. Arik, M. Arik, S. A. Cetin, T. Conka, A. Mailov, and S. Sultansoy, Eur. Phys. J. C **26**, 9 (2002).
[31] E. Arik, O. Cakir, S. A. Cetin, and S. Sultansoy, Phys. Rev. D **66**, 033003 (2002).
[32] E. Arik, O. Cakir, S. A. Cetin, and S. Sultansoy, Acta Phys. Pol. B **37**, 2839 (2006).
[33] W. S. Hou, A. Soni, and H. Steger, Phys. Lett. B **192**, 441 (1987).
[34] C. S. Huang, W. J. Huo, and Y. L. Wu, Mod. Phys. Lett. A **14**, 2453 (1999).
[35] A. Arhrib and W. S. Hou, Eur. Phys. J. C **27**, 555 (2003).
[36] T. M. Aliev, A. Ozpineci, and M. Savci, Eur. Phys. J. C **29**, 265 (2003).
[37] L. Solmaz, Phys. Rev. D **69**, 015003 (2004).
[38] A. J. Buras and M. Munz, Phys. Rev. D**52**, 186 (1995).
[39] Y. Nir, Phys. Lett. B **221**, 184 (1989).
[40] L. Wolfenstein, Phys. Rev. Lett. **51**, 1945 (1983).
[41] F. del Aguila, M. Perez-Victoria, and J. Santiago, J. High Energy Phys. 09 (2000) 011.
[42] A. Ali, E. Lunghi, C. Greub, and G. Hiller, Phys. Rev. D **66**, 034002 (2002).
[43] M. Blanke, A. J. Buras, S. Recksiegel, and C. Tarantino, arXiv:0805.4393.
[44] M. Beneke, F. Maltoni, and I. Z. Rothstein, Phys. Rev. D **59**, 054003 (1999).
[45] B. Aubert *et al.* (BABAR Collaboration), Phys. Rev. Lett. **93**, 011803 (2004).
[46] B. Aubert *et al.* (BABAR Collaboration), Phys. Rev. Lett. **93**, 081802 (2004).
[47] M. Iwasaki *et al.*, Phys. Rev. D **72**, 092005 (2005).
[48] E. Barberio *et al.* (Heavy Flavor Averaging Group), arXiv:0808.1297.
[49] T. E. Browder, T. Gershon, D. Pirjol, A. Soni, and J. Zupan, arXiv:0802.3201.
[50] M. Bona *et al.*, arXiv:0709.0451.